Annals of Oncology 27: 625–634, 2016
doi:10.1093/annonc/mdw007
Published online 17 January 2016

Identification of high-grade serous ovarian cancer miRNA species associated with survival and drug response in patients receiving neoadjuvant chemotherapy: a retrospective longitudinal analysis using matched tumor biopsies

M. Petrillo[1,†], G. F. Zannoni[2,†], L. Beltrame[3], E. Martinelli[2], A. DiFeo[4], L. Paracchini[3], I. Craparotta[3], L. Mannarino[3], G. Vizzielli[1], G. Scambia[1], M. D'Incalci[3*], C. Romualdi[5,‡] & S. Marchini[3,‡]

Departments of [1]Obstetrics and Gynaecology, Division of Gynaecologic Oncology; [2]Human Pathology, Catholic University of the Sacred Heart, Rome; [3]Department of Oncology, IRCCS Istituto di Ricerche Farmacologiche 'Mario Negri', Milan, Italy; [4]Case Comprehensive Cancer Center, Case Western Reserve University, Cleveland, OH, USA; [5]Department of Biology, University of Padova, Padova, Italy

Received 16 September 2015; revised 14 December 2015; accepted 7 January 2016

Background: Neoadjuvant chemotherapy (NACT) has been recognized as a reliable therapeutic strategy in patients with unresectable advanced epithelial ovarian cancer (EOC). The molecular events leading to platinum (Pt) response in NACT settings have hitherto not been explored. In the present work, longitudinal changes of miRNA expression profile were investigated to identify miRNA families with prognostic role in high-grade serous EOC patients who received the NACT regimen.

Patients and methods: One hundred sixty-four matched tumor biopsies taken at initial laparoscopic evaluation and at interval-debulking surgery (IDS) after four courses of Pt-based therapy were selected from 82 stage IIIC–IV high-grade serous-EOC patients that were judged unsuitable for complete primary debulking and subjected the NACT protocol. miRNA profiling by microarray, real-time PCR and immuno-histochemical staining for Smad2 phosphorylation (P-Smad2) were used for data analysis.

Results: Analysis revealed that 369 miRNAs were differentially expressed in matched biopsies (referred to as DEMs). DEMs were not scattered across the genome, but clustered into families: miR-199, let-7, miR-30, miR-181 and miR-29. Multivariate analysis showed that *miR-199a-3p*, *miR-199a-5p*, *miR-181a-5p* and *let-7g-5p* associated with overall and progression-free survival ($P < 0.05$); *miR-199a-3p*, *miR-199a-5p* and *miR-181a-5p* associated with residual tumor volume and Pt-free interval ($P < 0.05$). Immuno-histochemical staining confirmed an enrichment of P-Smad2, a marker of transforming growth factor-β activation, in tumors from patients with shorter PFS and OS, and with high levels of expression of *miR-181a-5p* ($P < 0.05$). Kaplan–Meier curves plotting concomitant expression of P-Smad2 and *miR-181a-5p* show significant differences in PFS and OS compared with those depicting the expression of each biomarker alone ($P < 0.001$).

Conclusions: This study describes several miRNA families with a prognostic role in the NACT setting. It also confirms that concomitant analysis of P-Smad2 and *miR-181a-5p* in surgical samples may be capable of identifying those ovarian cancer patients with poor outcome and little chance of response to Pt-based NACT.

Key words: high-grade serous ovarian cancer, neoadjuvant chemotherapy, longitudinal matched tumor biopsies analysis, *miR-181a-5p*

introduction

Although in high-grade serous-epithelial ovarian cancer (HGS-EOC), the evaluation of *BRCA1/2* mutational status has been recently recognized as a companion diagnostic tool for therapeutic decisions, the clinical management of EOC currently lacks reliable molecular and histological biomarkers that can guide therapeutic choices for the first and following therapies [1, 2]. Complete cytoreduction at the time of primary debulking surgery is currently considered as the goal to be pursued in the upfront management of women with advanced disease (National Comprehensive Cancer Network guidelines) [3]. In patients with unresectable disease, platinum (Pt)-based

*Correspondence to: Dr Maurizio D'Incalci, Department of Oncology, IRCCS Istituto di Ricerche Farmacologiche 'Mario Negri' Via La Masa 19, Milan 20156, Italy. Tel: +39-02-390141; E-mail: maurizio.dincalci@marionegri.it

†The first authors contributed equally to this work.
‡Both authors are last co-authors.

neoadjuvant chemotherapy (NACT) has emerged as a reliable therapeutic strategy. In particular, Pt-based NACT appears an attractive treatment option in women with extensive tumor burden since the vast majority of patients experience a relevant tumor shrinkage which allows complete interval debulking surgery (IDS) to be conducted after three to four courses of NACT. However, ~15%–20% of patients with advanced EOC do not respond to NACT [4] and present with progressively resistant disease ultimately dying within a few months after the initial diagnosis. These changes in the clinical response to chemotherapy probably mirror changes in the biology of tumor cells, a phenomenon known as 'temporal heterogeneity', which has been poorly investigated till now in HGS-EOC, since second surgery is uncommon in clinical practice.

Our group has recently dissected some features of temporal heterogeneity of EOC through the analysis of a cohort of patients from whom matched tumor biopsies were available at the time of primary surgery, before any treatment, and at time of relapse, after intervention with different lines of Pt-based chemotherapy [5]. We observed that cells from relapsed tumors had activated a transcriptional program led by transforming growth factor (TGF)-β and *miR-181a-5p*, which ultimately resulted in the transition from an epithelial to a mesenchymal state [6, 7]. Targeted re-sequencing analysis of genes involved in mechanisms controlling tumor cell growth, cell signaling and drug sensitivity showed that only 2% of somatic mutations observed at primary surgery were concordant in matched tumor biopsies from the same patients. Genomic and transcriptomic data suggest that the molecular portrait of cells from tumors of stage III–IV EOC at relapse, after one or more rounds of chemotherapy differ largely from that obtained at primary surgery, before chemotherapy [5].

The discovery of reliable biomarkers to predict response to Pt-based neoadjuvant therapy (NACT) and/or overall survival (OS) and progression-free survival (PFS) requires to identify first those genetic lesions that persist over time during therapy and that might confer a selective growth advantages to tumor cells.

In this study, we took advantage of a unique and homogenous cohort of tumor biopsies taken from patients who underwent NACT regimen, and from whom matched biopsies were available at initial laparoscopy surgery, before chemotherapy and at IDS after four cycles of Pt-based therapy. These samples allowed us two novel types of insights, first into changes in microRNA (miRNA) expression profiles related to mechanisms of response to carboplatin and taxol therapy, and second into any association between the expression of specific miRNAs and either patients' response to NACT or prognosis.

patients and methods

We retrospectively assessed 82 HGS-EOC patients, admitted between January 2004 and November 2011 at the Gynecologic Oncology Unit of the Catholic University of the Sacred Heart in Rome. Patients received an initial laparoscopic evaluation, with the assessment of Fagotti's score [8], and once judged unsuitable for optimal debulking surgery—due to the high tumor dissemination [9]—they were treated with NACT followed by IDS. The study has been carried out following the Declaration of Helsinki; the local scientific ethical committees approved the tumor sample collection and usage. Written informed consent was obtained from all patients. The study received the Institutional Review Board approval.

results

study design and patient characteristics

To assess at which degree NACT can modify the tumor miRNA landscape, analysis was carried out in a matched cohort of tumor biopsies taken from patients receiving NACT at initial laparoscopic exploration and at the time of IDS. The use of matched tumor biopsies provides the unique advantage of allowing identification of mechanisms of chemotherapy resistance characterized by similar features, irrespective of individual genetic variation. To further minimize parameters introducing variation, well-characterized stage III–IV tumors of the commonest histological subtype (serous papillary adenocarcinoma, 86.7%) and tumor grade (G3, 85.4%) were selected for the study. Histopathological and clinical features are summarized in Table 1. The median age at diagnosis was 62.5 years, with a median follow-up of 31 months; 44% of patients were alive and progression-free at the time of the last follow-up. All of them received the same schedule of Pt-based NACT (carboplatin AUC 5 plus paclitaxel 175 mg/m^2, every 3 weeks) with only some differences in term of duration of NACT regimen. In particular, we administered three cycles of NACT in 15 women (18.3%), and four cycles in 67 patients (81.7%). Recurrent disease was observed in the vast majority of patients (86.6%). Among them, 33% had a platinum-free interval (PFI) of >12 months and were therefore potentially sensitive to second-line Pt-based chemotherapy. Forty percent had a PFI of <6 months and were considered resistant to second-line Pt-based therapy, and 26.8% presented with a PFI between 6 months and 1 year and were considered partially sensitive. According to the Cox proportional hazard model analysis (Table 1) residual tumor after IDS (>1 cm) and PFI were significantly associated ($P < 0.05$) with both OS and PFS, whereas partial clinical response to NACT was associated to PFS only ($P = 0.04$).

miRNA landscape analysis

To identify the entire repertoire of miRNAs expressed in patients with stage III/IV EOC, we conducted microarray analyses. Initially, similarity across samples was investigated by unsupervised cluster analysis on the expression values of 457 miRNAs identified by miRNA landscape analysis at both initial laparoscopic biopsies and at IDS. The cluster depicted in Figure 1 (and reported in full scale in supplementary Figure S1, available at *Annals of Oncology* online) allowed unambiguous division of samples into two branches: branch I (green, on the left) composed of 57 biopsies and branch II (blue, on the right) composed of 107 biopsies (supplementary Table S1, available at *Annals of Oncology* online). There was no evidence of any association between these groups and survival measures, OS or PFS (data not shown). Next, we investigated whether initial laparoscopic samples and IDS biopsies from the same patient clustered close to each other or were intermingled across the two main branches of the cluster. Branch I was significantly enriched in initial laparoscopic biopsies ($P = 0.0001$), whereas branch II was enriched in IDS biopsies (supplementary Table S1, available at *Annals of Oncology* online).

Table 1. Clinical and histopathological features of the entire cohort of 82 patients enrolled in the study

Clinical annotations		*N* (%)	Progression-free survival		Overall survival	
			HR (95% CI)	*P*	HR (95% CI)	*P*
FIGO stage	III	65 (79.2)	–	–	–	–
	IV	17 (20.8)	1.00 (0.56–1.78)	0.98	1.27 (0.63–2.56)	0.51
Histotypes	Serous	71 (86.7)	–	–	–	–
	Endometrioid	3 (3.6)	0.81 (0.19–3.33)	0.77	0.57 (0.07–4.23)	0.59
	Indifferentiated	3 (3.6)	2.33 (0.71–7.58)	0.16	4.00 (1.21–13.71)	0.02
	Clear cell	4(4.9)	2.12 (0.65–6.85)	0.21	1.96 (0.61–6.37)	0.26
	Other	1 (1.2)	n.d.	n.d.	n.d.	n.d.
Grades	G1	2 (2.4)	–	–	–	–
	G2	9 (11.0)	1.68 (0.36–7.82)	0.51	1.24 (0.12–12.09)	0.85
	G3	70 (85.4)	1.38 (0.33–5.71)	0.65	2.76 (0.38–20.20)	0.32
	Missing	1 (1.2)	n.d.	n.d.	n.d.	n.d.
Relapsing[a]	No	11 (13.4)	–	–	–	–
	Yes	71 (86.6)	–	–	–	–
Residual Tumor	0 cm	69 (84.1)	–	–	–	–
	<1 cm	8 (9.7)	1.70 (0.80–3.58)	0.16	1.40 (0.54–3.59)	0.48
	>1 cm	5 (6.2)	28.16 (8.60–92.12)	<0.001	24.32 (7.43–79.59)	<0.001
PFI	≤6 months	33 (40.2)	–	–	–	–
	≤12 months	22 (26.8)	69.3 (13.6–351–9)	<0.001	3.12 (1.33–7.31)	0.008
	>12 months	27 (33.0)	220.5 (41.2–1179.5)	<0.001	13.88 (5.60–34.39)	<0.001
Vital status at the last follow-up[a]	Alive	36 (44.0)	–	–	–	–
	Dead	46 (56.0)	–	–	–	–
Ascites	No	13 (15.8)	–	–	–	–
	Yes	67 (81.8)	1.30 (0.68–2.51)	0.42	1.45 (0.64–3.29)	0.37
	Missing	2 (2.4)	n.d.	n.d.	n.d.	n.d.
Peritoneal carcinomatosis	Yes	79 (96.4)	–	–	–	–
	No	3 (3.6)	0.95 (0.23–3.93	0.95	0.44 (0.11–1.86)	0.27
Clinical response to NACT	Complete	10 (12.2)	–	–	–	–
	Partial	67 (81.7)	2.19 (1.30–4.61)	0.04	3.01 (0.93–9.89)	0.06
	Stable	4 (4.9)	2.38 (0.70–8.06)	0.16	4.58 (0.91–23.00)	0.06
	Progression	1 (1.2)	n.d.	n.d.	n.d.	n.d.
Pathological response to NACT	Partial Macro	46 (56.1)	–	–	–	–
	Partial Micro	27 (33.0)	0.71 (0.41–1.22)	0.22	0.84 (0.44–1.61)	0.60
	Stable	7 (8.5)	1.27 (0.56–2.89)	0.56	1.64 (0.62–4.33)	0.31
	Complete	1 (1.2)	n.d.	n.d.	n.d.	n.d.
	Progression	1 (1.2)	n.d.	n.d.	n.d.	n.d.
Number of NACT cycles	3	15 (18.3)	–	–	–	–
	4	67 (81.7)	–	–	–	–
Median CA-125		972	1 (0.99–1.01)	0.86	0.995 (0.99–1)	0.33
Median age [min–max] years		62.5 [31–83]	1 (0.98–1.10)	0.89	1.00 (0.98–1.03)	0.5
Median follow-up [min–max] months[a]		31 [1–144]	–	–	–	–
Total number of patients		82	–	–	–	–

[a]Survival-associated variables not used for survival analysis.
n.d., not determined.

These results are consistent with the hypothesis that tumor cells exposed to carboplatin plus taxol rapidly undergo dynamic molecular changes, so that several molecular features characterizing the tumor at primary surgery are modified by therapeutic intervention.

selection of miRNA families associated with modulation of platinum sensitivity

Next, matched tumor samples were analyzed for those miRNAs whose expression levels were either comparable between IDS and initial laparoscopic evaluation (−1.5<fold change<1.5, referred from now as CEM, *i.e.* comparable expressed miRNA) or different between the two groups (−1.5>fold change>1.5, referred from now on as DEM, *i.e.* differentially expressed miRNAs). We identified 369 miRNAs, 256 of which were CEM, and 113 of which were DEM (67 with a fold change>1.5 and 46 with a fold change<−1.5, supplementary Table S2, available at *Annals of Oncology* online). Unsupervised cluster analysis (supplementary Figure S2, available at *Annals of Oncology* online) depicted a complex and heterogeneous picture, suggesting that, despite the homogenous clinic-histological features and

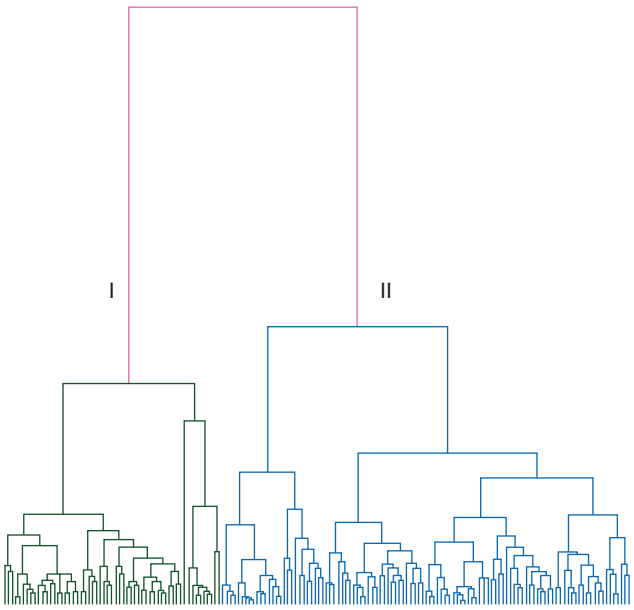

Figure 1. Unsupervised cluster analysis. Similarity across 82 HGS-EOC samples was investigated by unsupervised cluster analysis on the expression values of 457 miRNAs identified by miRNA landscape analysis at both initial laparoscopic biopsies and at IDS. Two different clusters were identified and labeled in green (cluster I) and in blue (cluster II).

treatment schedules of our cohort of patients, miRNA expression profiles poorly overlap in matched tumor biopsies. As the aim of our study was to identify miRNAs that correlate with response to standard Pt/taxol therapy, we started to analyze miRNAs which expression levels were comparable or increased between tumor cells at IDS versus initial laparoscopic biopsies, *i.e.* CEM and DEM with a fold change >1.5. The hypothesis is that cancer cells that are less sensitive to therapy maintain or increase their miRNA expression to confer a growth advantage. In contrast, DEM with a fold change<−1.5 are those miRNAs whose expression decreased in IDS versus initial laparoscopic evaluation, are probably involved in mechanism of cellular sensitivity and thus were excluded from downstream analysis. Applying this criterion, only 323 among the 369 miRNAs were selected for downstream analysis. Selected miRNAs were not scattered across the entire miRNome, but belonged to specific families. On the basis of their role in resistance against Pt as reported in the literature [10, 11], we focused our attention on five miRNA families: miR-199, miR-181, let-7, miR-29 and miR-30 (Table 2).

correlation of miRNA expression with clinical parameters

To investigate the potential correlation of five selected miRNAs families with clinical variables, we first validated microarray

Table 2. miRNA expression analysis and correlation with clinical parameters in multivariate analysis

miRNA family	Mature miRNA	IDS versus initial laparoscopic biopsy				Progression-free survival		Overall survival	
		Microarray		RT-PCR					
		logFC	*q*	Mean difference	*P*	HR (95% CI)	*P*	HR (95% CI)	*P*
hsa-miR-199	hsa-miR-199a-3p	1.58	<0.0001	18.51	<0.0001	1.92 (1.19–3.10)	0.006	2.91 (1.60–5.28)	0.0002
	hsa-miR-199a-5p	1.29	<0.0001	18.91	<0.0001	1.62 (1.1–2.61)	0.04	1.98 (1.1–3.56)	0.02
	hsa-miR-199b-5p	0.50	<0.0001	2.46	<0.0001	0.68 (0.41–1.11)	0.12	0.51 (0.27–0.92)	0.02
hsa-let-7	hsa-let-7b-5p	1.27	<0.0001	7.08	<0.0001	1.04 (0.65–1.68)	0.86	1.1 (0.59–1.89)	0.84
	hsa-let-7a-5p	1.51	<0.0001	2.21	<0.0001	1.83 (1.13–2.95)	0.01	1.61 (0.90–2.88)	0.10
	hsa-let-7c	1.49	<0.0001	18.86	<0.0001	0.89 (0.54–1.44)	0.62	1.1 (0.58–1.90)	0.87
	hsa-let-7e-5p	0.59	0.0001	15.18	0.277	1.1 (0.63–1.65)	0.94	1.18 (0.66–2.12)	0.56
	hsa-let-7f-5p	0.99	<0.0001	9.55	<0.0001	0.79 (0.49–1.27)	0.36	0.76 (0.42–1.38)	0.38
	hsa-let-7d-5p	0.57	<0.0001	4.18	0.0127	1.43 (0.89–2.30)	0.13	1.48 (0.82–1.66)	0.18
	hsa-let-7g-5p	1.04	<0.0001	10.38	<0.0001	1.84 (1.12–2.99)	0.01	1.82 (1.10–3.32)	0.04
	hsa-let-7i-5p	0.84	<0.0001	4.92	<0.0001	0.92 (0.57–1.49)	0.75	0.78 (0.43–1.41)	0.42
hsa-miR-29	hsa-miR-29a-3p	1.34	<0.0001	−0.03	0.9762	1.2 (0.74–1.92)	0.44	1 (0.56–1.74)	0.99
	hsa-miR-29b-3p	1.20	<0.0001	9.31	<0.0001	0.97 (0.60–1.56)	0.91	1.1 (0.61–1.92)	0.80
	hsa-miR-29c-3p	1.93	<0.0001	11.26	<0.0001	1.42 (0.89–2.27)	0.13	1.41 (0.78–2.51)	0.24
hsa-miR-30	hsa-miR-30c-5p	0.56	<0.0001	24.22	<0.0001	0.88 (0.54–1.41)	0.60	0.83 (0.46–1.48)	0.53
	hsa-miR-30b-5p	0.93	<0.0001	6.85	0.0001	1.1 (0.69–1.75)	0.69	1.33 (0.74–2.38)	0.33
	hsa-miR-30a-5p	0.75	<0.0001	0.43	0.1403	0.85 (0.53–1.35)	0.47	0.62 (0.34–1.13)	0.12
	hsa-miR-30d-5p	0.25	0.008	−0.76	0.1969	1 (0.65–1.69)	0.81	1.1 (0.58–1.86)	0.89
	hsa-miR-30e-5p	0.63	<0.0001	−3.95	0.5999	1.1 (0.63–1.62)	0.93	0.98 (0.55–1.76)	0.97
hsa-miR-181	hsa-miR-181a-5p	0.38	0.0008	2.08	0.1128	4.54 (2.63–7.83)	8.9E−09	4.37 (2.63–7.83)	5.8E−07
	hsa-miR-181b-5p	0.25	0.0008	−0.05	0.8013	1.1 (0.64–1.66)	0.83	1.11 (0.61–1.99)	0.72
	hsa-miR-181d	0.14	0.001	−9.02	0.1164	0.84 (0.52–1.34)	0.48	0.85 (0.48–1.53)	0.59

Summary table of miRNA family members selected for downstream signature validation and correlation with clinical parameters. For each miRNA, expression values obtained by microarray experiments (logFC, *q* value) and RT-PCR validation (mean difference, *P* value) is reported. Cox proportional hazards regression analysis of overall and progression-free survival for the 82 HGS-EOC patients is reported according to clinical variables described in Table 1. The hazard ratio (HR) is reported with its own 95% confidential interval (CI). *P* is the level of significance according to the Mann–Whitney *t*-test ($P < 0.05$). *q* is defined in supplementary Data, available at *Annals of Oncology* online.

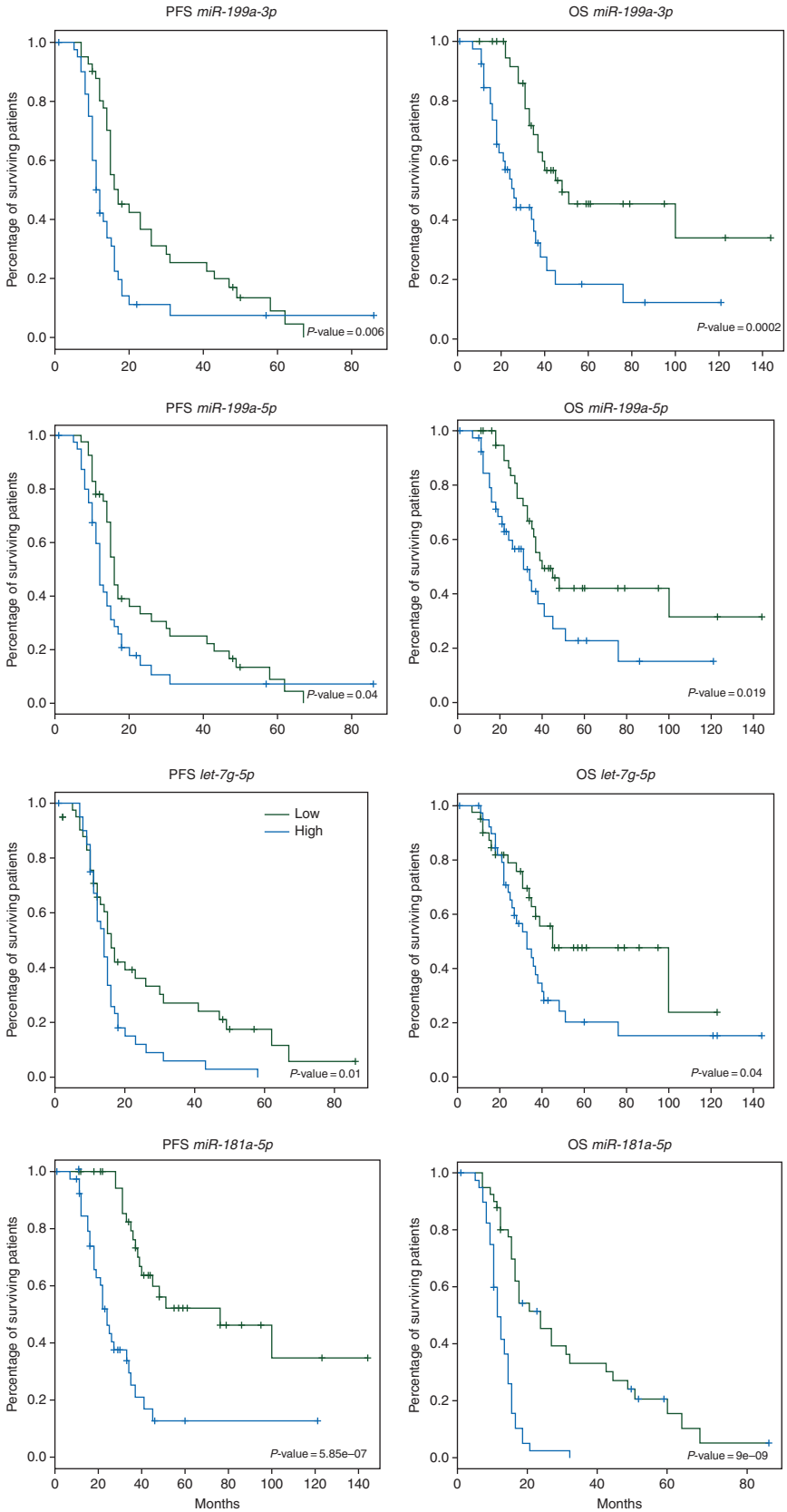

Figure 2. Kaplan–Meier curves of independent prognostic factors for OS and PFS. Figure shows the Kaplan–Meier curves of OS and PFS for *miR-199a-3p, miR-199a-5p, let-7g-5p, and miR-181a-5p* expression values in the entire cohort of 82 HGS-EOC patients who received neoadjuvant chemotherapy. miRNAs expression levels were converted into discrete variables by dividing the samples into two classes, high (blue) and low (green), under or over the cutoff points calculated as reported in supplementary Section 1 available at *Annals of Oncology* online. Results of log-rank test are added.

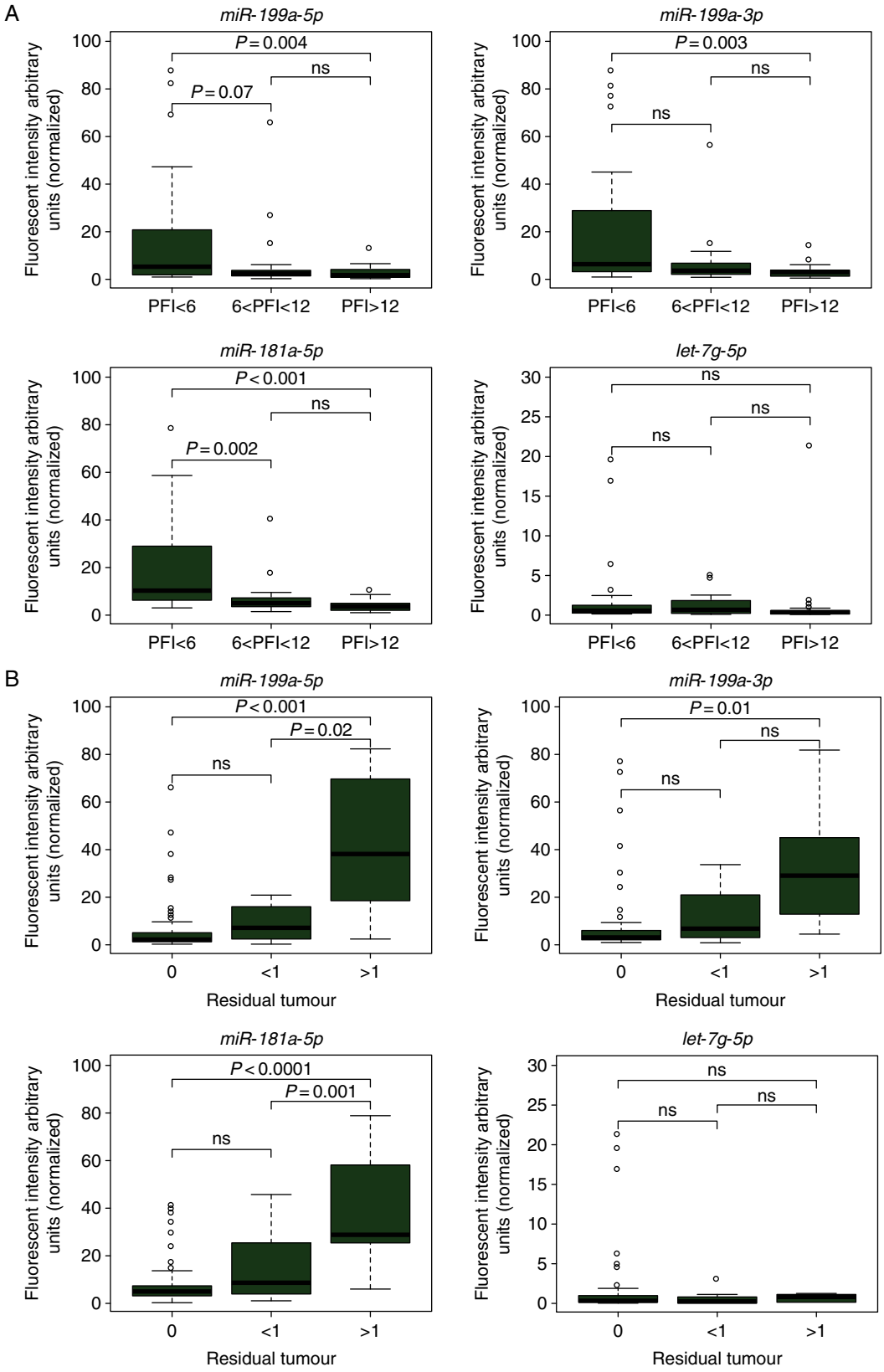

Figure 3. Association of *miR-199a-5p, miR-199a-3p, miR-181a-5p and let-7g* levels to PFI and residual tumor. Relative miRNA expression levels in patients tumor specimens with different time lagging the end of chemotherapy and first relapse (clinically defined as PFI) (A) or with different residual tumor after debulking surgery (B). Box plot diagrams show the expression levels of each miRNA measured by qRT-PCR in tumors biopsies. Within each box, the horizontal line indicates the median. The top edge of the boxes represents the 75th percentile, the bottom edge the 25th percentile. The range is shown as a vertical line ending above and below the 75th and 25th percentile values, respectively. *P*, level of significance according to t-test.

signatures by qRT-PCR. Data reported in Table 2 and in supplementary Figure S3, available at *Annals of Oncology* online, confirmed the robustness of our gene expression analysis, and thus worthy of downstream analysis.

Table 2 shows that among the miR-199 family members, *miR-199a-3p* and *miR-199a-5p* were associated with OS and PFS ($P < 0.005$), whereas *miR-199b-5p* was associated with OS only. Among the let-7 family members, *let-7a-5p* was associated with PFS ($P \leq 0.01$), whereas *let-7g-5p* was associated with OS ($P = 0.04$) and PFS ($P = 0.01$). No correlation was found for the other let-7 family members. As to the miR-181 family, *miR-181a-5p* had a strong association with OS ($P = 5.8\ e^{-7}$) and PFS ($P = 8.9\ e^{-9}$). None of the members of the miR-29 and miR-30 families were associated with OS or PFS (Table 2). Figure 2 shows survival plots for the prognostic groups identified by *miR-199a-3p, miR-199a-5p, let-7g-5p, miR-181a-5p*.

To examine the clinical relevance of the above selected four miRNAs, we analyzed their expression in patients tumors with different PFI or residual tumor after debulking surgery (Figure 3). The results suggest that tumor biopsies of patients with PFI <6 months, which is clinically defined as resistant to second-line Pt-based chemotherapy, presented with higher expression levels of miR-*181a-5p* ($P < 0.001$), *miR-199a-5p* ($P = 0.004$) and *miR-199a-3p* ($P = 0.003$) than patients with PFI between 6 and 12 months, which are clinically defined as partially sensitive to second-line Pt-based therapy or patients with PFI of >12 months (Figure 3A). No differences were observed for *let-7g-5p*. Furthermore, tumor biopsies taken from patients with residual tumor tissue after IDS of >1 cm displayed higher expression levels *of miR-181a-5p* ($P < 0.0001$), *miR-199a-5p* ($P < 0.001$) and *miR-199a-3p* ($P = 0.01$) than samples from the patients who lacked residual tumor or had residual tumor after IDS of <1 cm (Figure 3B). No differences were observed for *let-7g-5p*.

correlation of TGF-β pathway activation with prognosis

We have previously demonstrated that the expression of *hsa-miR-181a-5p* and Smad2 phosphorylation (P-Smad2), a marker of TGF-β pathway activation, stratifies patients in terms of risk of relapse and OS in a cohort of HGS-EOC [7]. In the light of these findings, we assessed levels of P-Smad2 in this NACT cohort. Figure 4A shows representative immunohistochemistry (IHC) staining for P-Smad2. Staining intensity and nuclear localization of P-Smad2 were not homogenous but varied among patients. Immuno-histochemistry scores in the patients' cohort ranged from 0 to 100, with a median of 60. Box plots (supplementary Figure S4, available at *Annals of Oncology* online) suggest that tumor biopsies taken from patients with PFI <6 months displayed more abundant nuclear P-Smad2 than biopsies obtained from patients with PFI >6 months. Instead, P-Smad2 levels were not different among patients with residual tumor <1 cm or >1 cm after debulking surgery.

Figure 4B (upper panels) reports Kaplan–Meier (KM) curves plotting OS and PFS against median tumor P-Smad2 histochemistry scores calculated for each patient. Data show a significant enrichment in P-Smad2, in patients who relapse within 20 months from the end of chemotherapy [$P < 0.001$; odds ratio (OR) = 1.4; 95% confidence interval (CI) 1.1–1.9] and have a short survival ($P < 0.001$; OR = 2.2; 95% CI 1.4–3.6). Intriguingly, KM curves of survival against concomitant expression of *miR-181a-5p* and immune score of P-Smad-2, stratified patients for risk of relapse and survival (Figure 4B, lower panels). This stratification was statistically more significant than that observed when survival was plotted against either biomarker alone (OS $P = 2.1e^{-12}$; PFS $P = 2.3e^{-11}$). In particular, we confirmed in this cohort of patients that, in tumors with both high miR-181a and high P-Smad2 expression, the median PFS was 10 months whereas, in patients with both low *miR-181a-5p* and P-Smad2, the median PFS was 22 months (OR = 12.5; 95% CI 5.6–27.9). Differences in OS were similar; patient tumors expressing high *miR-181a-5p* and P-Smad2 presented with a median OS of 16 months whereas, in patients with both low *miR-181a-5p* and P-Smad2, the median OS was 46.5 months (OR = 17.1; 95% CI 6.7–43.8). The PFS and OS for those patients with high *miR-181a-5p* and low P-Smad2 or vice versa were not significant (Figure 4B, lower panels).

We next assessed whether concomitant expression of *miR-181a-5p* and P-Smad2 was preferentially observed in tumor biopsies taken from patients with PFI > or <6 months or with residual tumor > or <1 cm. χ^2-test analysis (supplementary Table S3, available at *Annals of Oncology* online) revealed that co-expression of *miR-181a-5p* and P-Smad2 was more frequently observed in tumor biopsies taken from those patients with PFI <6 months than in tumor biopsies taken from those with PFI >6 months ($P = 2.65e^{-8}$). Moreover, tumor biopsies taken from patients with a residual tumor of >1 cm had higher expression levels of *miR-181a-5p* and P-Smad2 than tumor biopsies taken from those with a residual tumor of <1 cm ($P = 0.013$, supplementary Table S3, available at *Annals of Oncology* online).

Using Cox proportional multivariate survival model, we evaluated the best predictive covariates among those identified including *let-7g-5p*, *miR-181a-5p*, *miR-199a-3p*, *miR-199a-5p*, P-Smad2, clinical response to NACT and residual tumor after IDS. Table 3 shows that P-Smad2, *miR-181a-5p* and clinical response to NACT are the three covariates that most aptly identify the risk of patients relapse or death. *let-7g-5p* was associated with OS [hazard ratio (HR) 1.1, 95% CI 1.04–1.23, $P = 0.0021$], and residual tumor after IDS >1 cm was associated with PFS (HR 7.33, 95% CI 1.5–38.85, $P = 0.01$). No association was observed for the miR-199a family members (Table 3).

discussion

In this study, the longitudinal analysis of the miRNA expression profile in HGS-EOC patients who received NACT helped to pinpoint miRNAs involved in the early mechanisms of Pt-based resistance that might be of potential clinical utility as biomarkers of poor prognosis. We gained two insights: (i) expression levels of miRNA *let-7g-5p*, *miR-199a-3*p, *miR-199a-5p* and *miR-181a-5p* at diagnosis were independently associated with OS and PFS. (ii) Concomitant expression of P-Smad2 and *miR-181a-5p* was related to poor prognosis, residual tumor after IDS and survival.

This is, to our knowledge, the first study demonstrating, in matched HGS-EOC tumor biopsies, the expression levels of

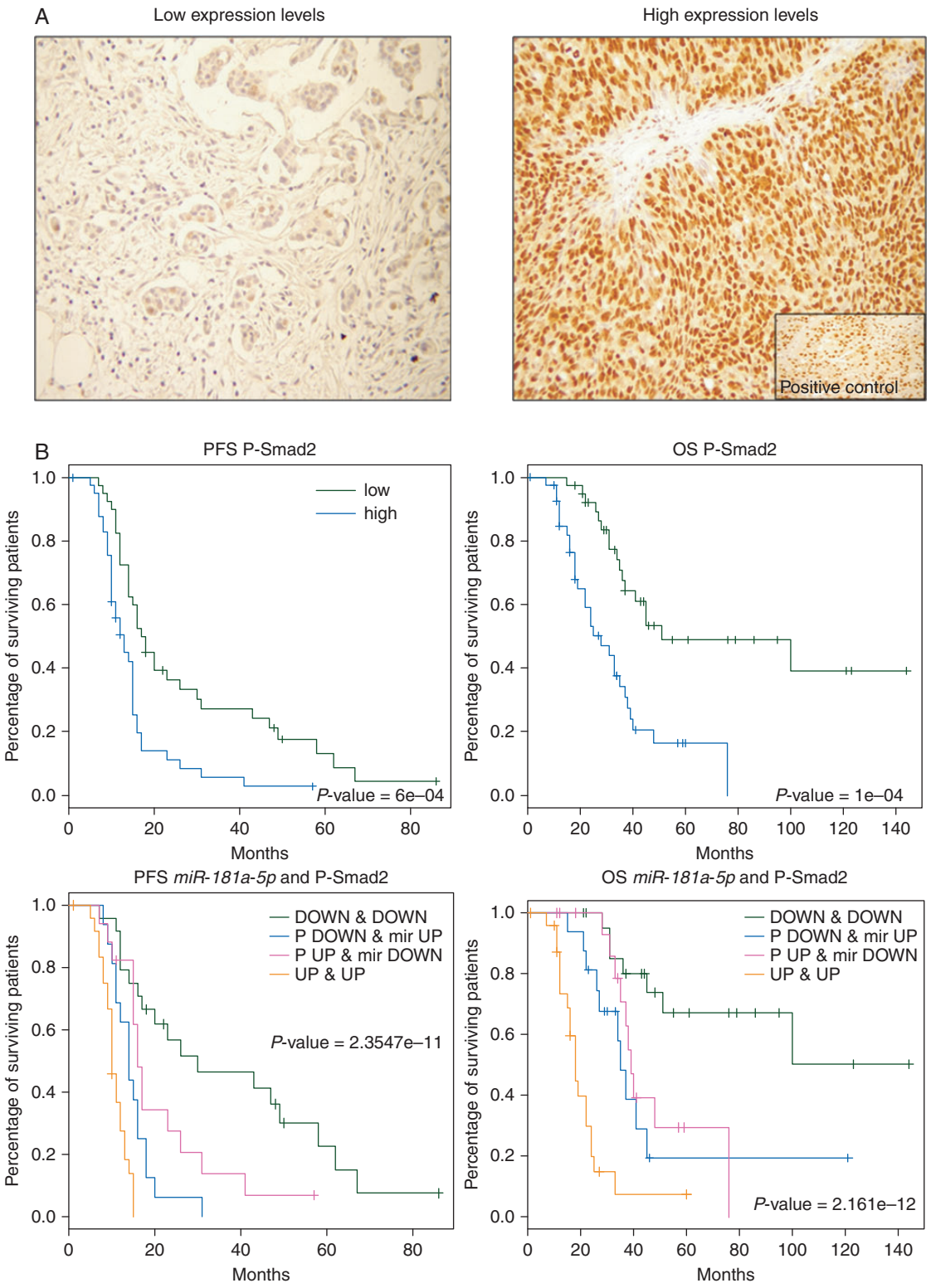

Figure 4. *miR-181a-5p* and P-Smad2 correlation with clinical parameters. (A) Representative IHC analysis for nuclear P-Smad2. The analysis of all tissue sections was done, without any prior knowledge of clinical parameters, by two authors (GFZ, EM), by means of light microscopy. The percentage of immunostained tumor cells was assessed at low magnification (×5 objective lens) by evaluating the entire tumor area, and it was expressed as percentage of positive cells. A positive control image is reported in the box. (B) *miR-181a-5p* and P-Smad2 correlation with clinical parameters. Upper panel: Kaplan–Meier curves derived from dichotomizing P-Smad-2 expression at the median OS and PFS. Lower panel: OS and PFS outcomes in concomitant *miR-181a-5p* and P-Smad2 expression. Statistical significance was assessed for differences in PFS and OS in patients samples with concomitant decrease versus increase in *miR-181a-5p* and P-Smad2 expression, compared with each biomarker alone.

Table 3. Multivariate analysis

miRNA	Overall survival		Progression-free survival	
	HR (95% CI)	*P*	HR (95% CI)	*P*
hsa-let-7g-5p	1.1 (1.04–1.23)	0.0021	1 (0.97–1.1)	0.21
hsa-miR-181a-5p	1.1 (0.99–1.12)	0.03	1.1 (1.04–1.2)	0.003
hsa-miR-199a-5p	1.03 (0.97–1.1)	0.62	0.98 (0.93–1.1)	0.88
hsa-miR-199a-3p	0.99 (0.95–1.02)	0.32	0.99 (0.95–1.1)	0.23
P-Smad2	1.1 (1.0–1.2)	0.006	1.1 (1–1.2)	0.04
Clinical response to NACT				
Complete	–	–	–	–
Partial	2.0 (0.61–6.85)	0.24	2.03 (0.94–4.38)	0.07
Stable	1.93 (0.34–11.05)	0.46	1.12 (0.27–4.61)	0.86
Progression	24.91 (1.15–138–16)	0.04	56.69 (1.67–1924.64)	0.02
Residual tumor				
0 cm	–	–	–	–
<1 cm	1.52 (0.55–4.22)	0.73	1.2 (0.53–2.78)	0.65
>1 cm	0.99 (0.08–11.80)	0.42	7.33 (1.50–35–85)	0.01

Cox proportional hazards regression analysis of overall and progression-free survival for the 82 HGS-EOC patients is reported according to clinical variables described in Table 1 and molecular signatures previously identified. The hazard ratio (HR) is reported with its own 95% confidential interval (CI). *P*, significance level according to Cox proportional hazard model.

the above-mentioned four miRNAs associated with Pt-response and prognosis. We observed that *miR-181a-5p*, *miR-199a-5p* and *miR-199a-3p* were more expressed in tumors of patients with PFI <6 months, with residual tumor >1 cm, and their expression levels were associated to patients' survival. Characterization of the molecular mechanisms via which these four miRNAs might be involved in Pt-based resistance is beyond the scope of this work. Nevertheless, some hypotheses can be discussed taking into account the data published so far. The current knowledge of the roles of these miRNAs is limited [12]. However, Yang et al. identified a subset of miRNAs and genes that once integrated into a mesenchymal signature (IM) are associated with poorer prognosis in HGS-EOC than genes integrated into the epithelial signature (IE) [11]. miR-199 family members were upregulated in the IM signature compared with the IE signature. Our analysis is consistent with the notion that high tumor levels of miR-199 family members correlated with poor prognosis. Our group demonstrated that, in stage I tumor biopsies, the expression levels of *miR-199a-3p* and *miR-199a-5p* were associated with poor prognosis [13]. Thus, it is plausible to speculate that, although stage I and stage III represent different diseases, they share the same anatomical site of growth and proliferation (*i.e.* the ovary) as well as the molecular mechanisms which confer resistance against front-line Pt-based chemotherapy. Information on levels of *let-7* members in HGS-EOC is unavailable. This is relevant as they have been suggested to act as tumor suppressors [12, 14, 15]. However, further analysis in independent validation sets is required to consider *miR-199a-3p*, *miR-199a-5p*, and *let-7g-5p* as prognostic markers for HGS-EOC.

As far as the second insight, the association of concomitant expression of P-Smad2 and *miR-181a-5p* to poor prognosis, residual tumor after IDS and survival results confirms our previous preliminary findings, strengthening the potential clinical relevance of this miRNA. [7]. We have previously demonstrated that patients with high expression levels of *miR-181a-5p* at diagnosis relapsed within 6 months from the end of Pt-based therapy with a relatively short survival [7]. Instead, patients with low levels of *miR-181a-5p* relapsed after 6 months from the end of chemotherapy and had a good prognosis. As to the potential biological mechanisms, we demonstrated that *miR-181a-5p* controls the activity of the TGF-β pathway, by directly downregulating the expression levels of Smad-7, an intracellular inhibitor of TGF-β. In various *in vitro* and *in vivo* models, enhanced expression of *miR-181a-5p* led to increased cellular motility, dissemination and resistance to therapy, due to cellular transition from an epithelial state to a mesenchymal state (EMT). To demonstrate the role of *miR-181a-5p* and EMT in driving Pt resistance in relapsed tumors, expression levels of *miR-181a-5p* and of selected EMT markers were compared in a second and independent cohort of tumor biopsies, taken from patients before chemotherapy, when the tumor was Pt sensitive, and at relapse, after many lines of chemotherapy when the tumor had acquired resistance. Data from matched human biopsies mirrored the *in vitro* models: *miR-181a-5p* expression levels were increased in relapsed resistant tumors compared with paired primary sensitive tumors. The same results were obtained for the other markers associated with the EMT and controlled by the TGF-β receptor.

Although in this study biopsies came from NACT-treated patients, which is a quite different clinical situation from that previously described [7], results strengthened our hypothesis that *miR-181a-5p* is an 'oncomiR' in HGS-EOC. By regulating the TGF-β pathway, *miR-181a-5p* confers a positive advantage to tumor cells to withstand Pt treatment.

One might hypothesize that, for biomarker identification within the complex and heterogeneous genetic background of HGS-EOC, pathway-based approaches may perform better than single-gene approaches. Our previous study revealed that combined genomic and proteomic analysis of biomarkers that

regulate the EMT process provides a more functionally relevant prognostic signature than analysis of each biomarker alone [7]. In line with these data, KM curves combined by plotting the expression levels of both *miR-181a-5p*-known to increase the TGF-β signaling by shutting down the negative regulatory protein Smad-7-with the nuclear P-Smad2 protein—a nuclear protein that is phosphorylated upon activation of the TGF-β pathway-carried out better than curves considering the expression of each biomarker alone. In conclusion, since these findings represent a second independent validation of previous findings [7], our data strongly indicate that at least two key elements of the TGF-β pathway, i.e. *miR-181a-5p* and P-Smad2, allow us to identify those patients who will not benefit from the standard protocols of Pt-based NACT and thus should be treated with novel investigational drugs or new combinations. The involvement of TGF-β and EMT in the resistance to conventional therapy provides a valid rational to investigate new drugs that target this pathway.

acknowledgement

We thank Andreas Gescher (Leicester, UK) for critical revision and editing of the manuscript. Nerina and Mario Mattioli Foundation, ACTO Foundation, Cloud4CaRe program.

funding

This work was supported by Italian Association for Cancer Research (grant number IG15177 to SM and IG17185 to CR) and Cariplo Foundation (grant number, 2013-0815 to SM and CR).

disclosure

The authors have declared no conflicts of interest.

references

1. Bast RC, Jr, Hennessy B, Mills GB. The biology of ovarian cancer: new opportunities for translation. Nat Rev Cancer 2009; 9: 415–428.
2. Ledermann J, Harter P, Gourley C et al. Olaparib maintenance therapy in patients with platinum-sensitive relapsed serous ovarian cancer: a preplanned retrospective analysis of outcomes by BRCA status in a randomised phase 2 trial. Lancet Oncol 2014; 15: 852–861.
3. Bristow RE, Chang J, Ziogas A et al. Impact of National Cancer Institute Comprehensive Cancer Centers on ovarian cancer treatment and survival. J Am Coll Surg 2015; 220: 940–950.
4. Vergote I, Trope CG, Amant F et al. Neoadjuvant chemotherapy is the better treatment option in some patients with stage IIIc to IV ovarian cancer. J Clin Oncol 2011; 29: 4076–4078.
5. Beltrame L, Di Marino M, Fruscio R et al. Profiling cancer gene mutations in longitudinal epithelial ovarian cancer biopsies by targeted next-generation sequencing: a retrospective study. Ann Oncol 2015; 26: 1363–1371.
6. Marchini S, Fruscio R, Clivio L et al. Resistance to platinum-based chemotherapy is associated with epithelial to mesenchymal transition in epithelial ovarian cancer. Eur J Cancer 2013; 49: 520–530.
7. Parikh A, Lee C, Joseph P et al. microRNA-181a has a critical role in ovarian cancer progression through the regulation of the epithelial-mesenchymal transition. Nat Commun 2014; 5: 2977.
8. Fagotti A, Vizzielli G, De Iaco P et al. A multicentric trial (Olympia-MITO 13) on the accuracy of laparoscopy to assess peritoneal spread in ovarian cancer. Am J Obstet Gynecol 2013; 209: 4–62.
9. Vizzielli G, Costantini B, Tortorella L et al. Influence of intraperitoneal dissemination assessed by laparoscopy on prognosis of advanced ovarian cancer: an exploratory analysis of a single-institution experience. Ann Surg Oncol 2014; 21: 3970–3977.
10. Network TCGAR. Integrated genomic analyses of ovarian carcinoma. Nature 2011; 474: 609–615.
11. Yang D, Sun Y, Hu L et al. Integrated analyses identify a master microRNA regulatory network for the mesenchymal subtype in serous ovarian cancer. Cancer Cell 2013; 23: 186–199.
12. Zaman MS, Maher DM, Khan S et al. Current status and implications of microRNAs in ovarian cancer diagnosis and therapy. J Ovarian Res 2012; 5: 44.
13. Marchini S, Cavalieri D, Fruscio R et al. Association between miR-200c and the survival of patients with stage I epithelial ovarian cancer: a retrospective study of two independent tumour tissue collections. Lancet Oncol 2011; 12: 273–285.
14. Tang Z, Ow GS, Thiery JP et al. Meta-analysis of transcriptome reveals let-7b as an unfavorable prognostic biomarker and predicts molecular and clinical subclasses in high-grade serous ovarian carcinoma. Int J Cancer 2014; 134: 306–318.
15. Boyerinas B, Park SM, Murmann AE et al. Let-7 modulates acquired resistance of ovarian cancer to Taxanes via IMP-1-mediated stabilization of multidrug resistance 1. Int J Cancer 2012; 130: 1787–1797.